Journal of Thermal Analysis and Calorimetry, Vol. 69 (2002) 751–771

OXIDE MELT SOLUTION CALORIMETRY OF RARE EARTH OXIDES
Techniques, problems, cross-checks, successes

K. B. Helean and A. Navrotsky[*]

Thermochemistry Facility, Department of Chemical Engineering and Materials Science University of California at Davis, Davis, CA 95616, USA

Abstract

Key to the evaluation of the long-term durability and reactivity of REE-materials is the accurate determination of their thermodynamic properties. High-temperature oxide melt solution calorimetry offers an effective methodology for the determination of enthalpies of formation for REE-materials. Calorimetric techniques and crosschecks are summarized that demonstrate that consistent and correct thermodynamic data can be generated using lead borate and sodium molybdate solvents. A summary of recent calorimetric studies of REE-orthophosphates and REE-oxyapatites illustrates the successful application of our techniques in quantifying formation enthalpies and elucidating energetic trends.

Keywords: oxide melt solution calorimetry, rare earth oxides

Introduction

Rare earth elements (REE), the lanthanides plus yttrium, play an important role as trace element indicators of geochemical processes [1–5]. As such, the behavior of REE in hydrothermal and magmatic settings has been extensively investigated (over 2700 references in GEOREF [6]). REE usefulness stems from their chemical properties, which vary systematically as a function of atomic number. As the inner 4*f* orbital is filled with electrons across the lanthanide series, (La $4f^{0}$ to Lu $4f^{14}$), a smooth contraction of the ionic radius occurs [7]. This results in a series of elements with differing degrees of crystal chemical incompatibility with most earth forming minerals. Igneous petrologists, therefore, can use REE partition coefficients, to unravel the petrogenesis of igneous rocks [8]. By examining the Eu and Ce oxidation states, geochemists can deduce the redox conditions of the formation of rocks and sediments [9, 10]. REE are particularly useful as geochemical tracers in the study of the cosmos [10–14]. Due to their refractory nature, no significant REE fractionation due to volatility is presumed to have occurred during the formation of the earth. By comparing REE ratios in terrestrial and extraterrestrial rocks, formation temperatures for meteorites can be constrained.

---

[*] Author for correspondence: E-mail: anavrotsky@ucdavis.edu

1418–2874/2002/ $ 5.00

Akadémiai Kiadó, Budapest
Kluwer Academic Publishers, Dordrecht

REE-compounds are used widely in technological applications. Zirconia, ZrO_2, when doped with REE, e.g. yttrium stabilized cubic zirconia (YSZ), becomes an oxygen ion conductor allowing its use as a solid oxide fuel cell, oxygen sensor, oxygen pump and exhaust catalyst [15–17]. REE-doped zirconia and orthophosphates are also used as an inert matrix for mixed oxide nuclear fuels (MOX) REE oxides comprise 50 percent by mass of this fuel designed to burn excess weapons plutonium in modified reactors [18–20]. REE compounds, such as doped La_2MnO_4 and $Gd_2Ti_2O_7$, are giant magneto-resistors [21]. REE-orthophosphates such as monazite, $LaPO_4$, are used for their luminescence and lasing properties [22–24]. REE are important dopants in the ceramic processing of silicon nitrides [25]. REE from Nd to Lu are produced during fission of ^{235}U and during the radioactive decay of ^{238}U and ^{239}Pu [26]. As a result, the REE content will grow over time in any waste form.

Key to the evaluation of REE geochemical models and the assessment of long-term durability and reactivity of REE-materials, including actinide host phases, is the accurate determination of their thermodynamic properties, such as enthalpies of formation. REE-oxide and nitride compounds are highly refractory, making them particularly useful in high-temperature applications. This is also the physical property that precludes the measurement of their formation enthalpies using standard aqueous acid calorimetry. High-temperature oxide melt solution calorimetry offers an alternative and more effective methodology [27, 28]. Reactants and products are each dissolved in a molten oxide solvent, usually at 976 or 1078 K, to produce a dilute solution. In order for this technique to produce reliable results, the final state of the REE and other solutes in the solvent must be reproducible. No precipitates or secondary phases should form during the experiments and dissolution of samples should be complete and reasonably rapid. The refractory nature of rare earth oxides makes these conditions harder to attain and verify than is the case for compounds containing oxides of the alkalis, alkaline earths, silicon, aluminum, or transition metals. This paper summarizes recent work in the UC Davis Thermochemistry Facility that demonstrates through a series of thermodynamic cross-checks that the final state of REE in lead borate and sodium molybdate solvents is reproducible and that consistent and correct thermochemical data can be generated. Calorimetric protocols are recommended for future studies of REE-materials.

Calorimetric procedures and possible problems with REE-bearing materials

Details of the twin Calvet microcalorimeter and data collection procedures have been published elsewhere [27, 28]. These references also discuss appropriate calibration procedures. We currently have calorimeters operating continuously near 976 and 1078 K.

Transposed temperature drop calorimetry (TTD)

In the TTD experiment, a pelletized powdered sample is dropped into a hot calorimeter in the absence of solvent. The heat effect is equal to the heat content of the sample,

$\int_{298}^{T} C_p \mathrm{d}T$, if no phase transformation or decomposition occurs. For hydrous or carbonated REE-compounds, the TTD experiment yields the heat content plus the enthalpy of decomposition. With a gas (N_2, Ar, O_2, or air) flowing through the calorimeter, a reproducible calorimetric final state is attained [29].

Drop solution calorimetry (DS)

The second type of experiment, drop solution (DS) calorimetry, involves dropping a sample pellet from room temperature into a solvent held at calorimeter temperature. The heat effect is equal to the heat content plus the enthalpy of solution at calorimeter temperature, $\Delta H_{ds} = H_s + \int_{298}^{T} C_p \mathrm{d}T$. Complications may include incomplete dissolution or reaction with the solvent to form a metastable compound due to local saturation of the melt. Such side reaction leads to an irreproducible final state. Two different solvents have been used, $3Na_2O{\cdot}4MoO_3$ at 976 K and $2PbO{\cdot}B_2O_3$ at 976 and 1078 K. The lead borate solvent quenches to a glass. This makes a direct examination of the solvent using optical microscopy or electron probe microanalysis possible. Such analysis is much more difficult with the sodium molybdate solvent as it solidifies into a multi-phase crystalline assemblage. Therefore the REE distribution in the solidified solvent bears little relation to the REE environment in the melt. Thermodynamic cross-checks can be used to verify that the use of sodium molybdate solvent is appropriate for the study of REE-materials.

Previous DS studies of REE-oxides used $2PbO{\cdot}B_2O_3$ at 976 K with gas bubbled through the solvent to agitate the melt and aid in dissolution [30, 31]. The difficulties in dissolving REE_2O_3 were addressed by using a dispersant such as SiO_2 or solidified solvent to minimize local saturation at the surface of the dissolving pellet [32, 33]. The dispersant method increases the error associated with sample mass if the mixture is not perfectly homogeneous. Error is also increased because a large part of the heat effect is attributed to the dispersant but all of the uncertainty is propagated into ΔH_{ds} for the sample. Direct examination of the quenched lead borate glass after dissolving Y_2O_3+$2PbO{\cdot}B_2O_3$ pellets suggested that this method was effective in achieving complete dissolution at 976 K with no detectable Y-borate compound formation [33].

Ternary compounds in which REE oxides are dispersed with other elements on the atomic scale often dissolve more rapidly, and with less local saturation, than the REE_2O_3 materials themselves. Thus DS of such ternary compounds in $2PbO{\cdot}B_2O_3$ is often possible near 976 as well as 1078 K. Once the ΔH_{ds} of the binary oxides is well established at both temperatures, which is a goal of the present work, the enthalpies of formation of REE-containing ternary compounds and of glasses can often be measured using DS calorimetry in $2PbO{\cdot}B_2O_3$ at either temperature.

Solution calorimetry (S)

The third calorimetric method is solution calorimetry [27, 28]. A sample is equilibrated in a sample cup above the solvent in the calorimeter. In order for this method to work, the sample must not react with the solvent vapors or undergo decomposition or phase change as a result of prolonged exposure to calorimetric temperatures. Solution calorimetry is slower and more laborious than drop solution calorimetry because, in the former, the sample assembly must be changed after each dissolution, while, in the latter, several pellets can often be dropped successively. However solution calorimetry has certain advantages. In some cases the heat content of the sample, which is always endothermic, is offset by an exothermic enthalpy of solution of the same magnitude. Then the enthalpy of drop solution is nearly zero. Such a small heat effect is hard to measure accurately because of the difficulty in deciding when the reaction returns to baseline. In other cases, a pressed pellet does not dissolve adequately in the solvent of choice, but powdered sample dissolves more readily. A detriment of solution calorimetry is the need to correct the data for heat effects associated with stirring. This stirring effect results both from friction and from moving mass (the sample cup and its attached silica glass manipulation rod) through the small temperature gradient of the calorimeter furnace.

The standard solution calorimetry technique utilizes a sample cup with drainage holes in the bottom (Fig. 1) [28, 29]. Once the sample powder is thermally equilibrated, in approximately seven hours, the sample cup is lowered and the sample is mechanically

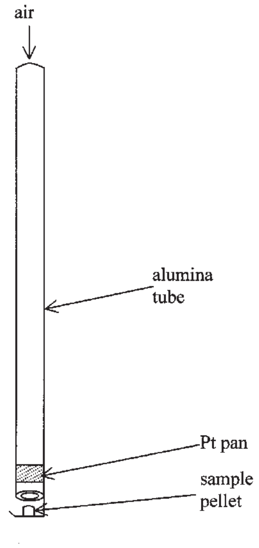

Fig. 1 Schematic of the airgun 'solution' calorimetry sample holder. A pellet of material is suspended over solvent at calorimeter temperature until thermal equilibration. A burst of air through the alumina tube dislodges the pellet from the Pt pan and it falls into the solvent. In this manner an enthalpy of solution, ΔH_s, is measured

stirred into the solvent. The heat generated during this experiment represents the enthalpy of solution plus the enthalpy of the mechanical stirring. Blank experiments are conducted to measure the stirring correction. A slight modification of the standard solution calorimetry sample holder has been made recently and is shown for comparison in Fig. 1.

We have developed a new solution technique referred to as the 'airgun' technique [34]. This avoids the need to correct the data for a stirring effect. A pellet of sample is placed into a Pt pan attached to the end of an alumina tube (Fig. 2). The assemblage is lowered into the calorimeter such that the pellet sits just above the solvent. The calorimeter is monitored until a stable baseline is achieved, typically the equilibration time is 1.5 h. The pellet is then dislodged from the pan by a small burst of air through the alumina tube. The resulting calorimetric signal consists of only the enthalpy of solution, ΔH_{ds}. Obviously, the pelletized sample must dissolve well for this method to be effective.

A previous study of REE_2O_3 dissolution in $2PbO{\cdot}B_2O_3$ at 975 K used the standard solution calorimetry technique with powdered samples [35]. Their data are discussed in

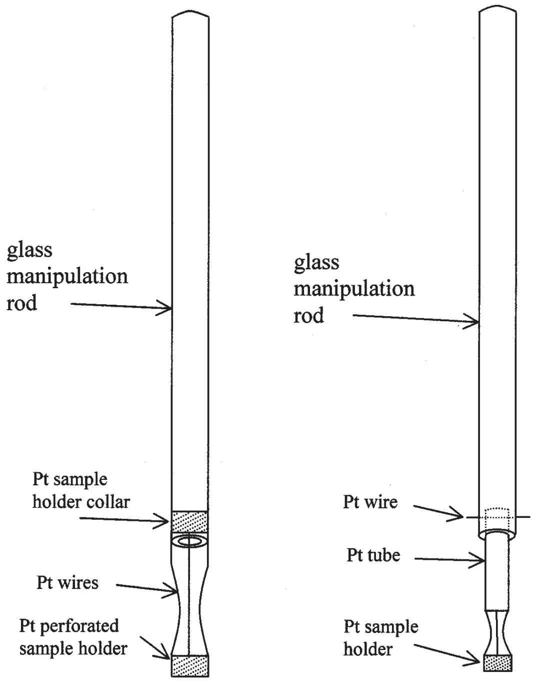

Fig. 2 Schematic of the standard solution calorimetry sample holder (left) and a slight modification using tubing instead of wires to ease alignment (right). In both cases powdered material is suspended over solvent in a sample cup with a perforated Pt foil bottom at calorimeter temperature until thermal equilibration (approximately seven hours or over night). The sample cup is manually lowered and the sample is mechanically stirred into the solvent. The calorimeter signal for these solution experiments consists of ΔH_s and ΔH_{stir}

detail below and compared to ΔH_s values calculated using drop solution data and heat contents. Another previous study of REE_2O_3 using the solution calorimetry technique addressed the dissolution difficulties in a unique way [36]. A 'fluffy' oxide was precipitated by dissolving the REE_2O_3 sample in nitric acid and then precipitating a high-surface area sample with the addition of aqueous ammonia. This porous material allowed ready access of solvent. Possible complications are the introduction of impurities into the sample. Questions may arise as to the structural state and surface area of the starting material. Careful structural and chemical analysis of the 'fluffy' oxide is essential.

Furnace tests and electron microprobe analysis of quenched $2PbO{\cdot}B_2O_3$ solvents

Furnace tests are conducted to evaluate the dissolution of pellets in the solvent of choice. A pellet, typically 5 mg, is dropped into approximately 5 g of molten solvent at calorimeter temperature. This maintains the approximate ratio of sample to solvent expected over the course of a series of drop solution experiments. The melt, after a given period of time, is poured into an inert dish (quenched), and then examined by visual, microscopic, and analytical techniques.

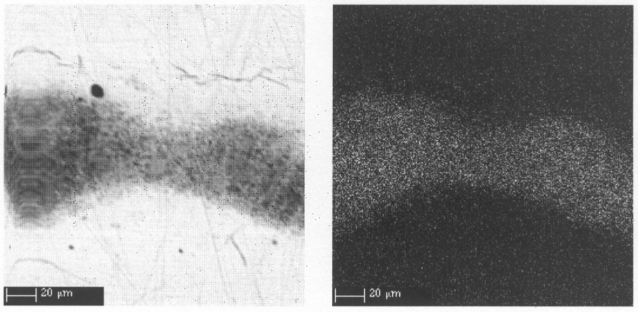

Fig. 3 BSE micrograph (left) and La *L*α X-ray dot map (right) of an undissolved La_2O_3 particle. The matrix is $2PbO{\cdot}B_2O_3$ solvent quenched after one hour at 975 K

Electron microprobe analysis (EMPA) has been used to test whether dissolution of La_2O_3 and Y_2O_3 was complete in experiments using $2PbO{\cdot}B_2O_3$ solvent. Back scattered electron (BSE) imaging and energy dispersive spectrometry (EDS) were used to examine the solvents quenched from furnace tests. Three sets of furnace experiments were conducted. The first consisted of dropping approximately 5 mg pellets of either La_2O_3 or Y_2O_3 into 5 g of molten $2PbO{\cdot}B_2O_3$ at 976 K and holding at temperature for one hour, the upper limit of acceptable reaction duration. The solvent was quenched into a graphite dish. The resulting glasses were polished, carbon coated and subjected to EMPA-BSE and EDS. Fragments of undissolved La_2O_3 and Y_2O_3 were seen (Figs 3 and 4). This is consistent with previous observations that dissolution of REE_2O_3 pellets in $2PbO{\cdot}B_2O_3$ solvent at 976 K was sluggish and often incomplete [33, 36]. The second test was identi-

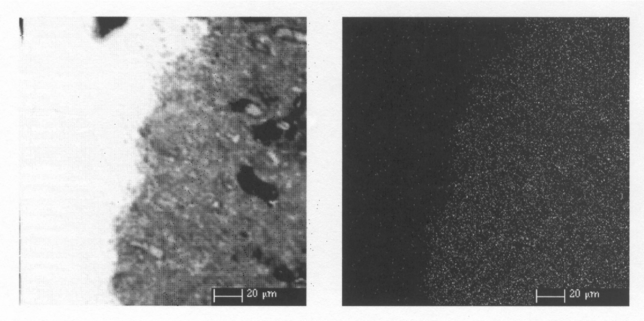

Fig. 4 BSE micrograph (left) and Y *L*α X-ray dot map (right) of an undissolved Y_2O_3 particle. The matrix is $2PbO{\cdot}B_2O_3$ solvent quenched after one hour at 975 K

cal to the first except that the temperature was raised to 1078 K. No undissolved fragments of pellet were observed. An X-ray dot map of the solvent indicated that the Y and La were homogeneously distributed. These results verify that dissolution of La_2O_3 and Y_2O_3 pellets in $2PbO{\cdot}B_2O_3$ at 1078 K was achieved. The third set of experiments simulated solution calorimetry in that the La_2O_3 and Y_2O_3 were not pelletized. Approximately 5 mg of powder was dropped into $2PbO{\cdot}B_2O_3$ solvent at 976 K and held at temperature for one hour. EMPA-BSE of the quenched solvent showed no undissolved particles. Apparently for La_2O_3 and Y_2O_3 increasing the sample surface contact with the solvent is sufficient to achieve dissolution in $2PbO{\cdot}B_2O_3$ solvent at 976 K. This verifies the technique used by Takayama-Muramachi and Navrotsky [35]. These results combined with the calorimetric results are taken as evidence that dissolution of all REE_2O_3 pellets in lead borate at 1078 K was achieved.

Summary of calorimetric data for REE oxides

Heat content measurements for REE_2O_3

Transposed temperature drop (TTD) calorimetry was used to measure the heat contents, $H_{975}-H_{298}$, of six REE-sesquioxides. They were compared to calculated values using reference heat capacity equations [37] (Table 1). The measured values were, within error, equal to the tabulated values. The excellent agreement confirmed that our handling of the REE_2O_3 resulted in no significant contamination by H_2O or CO_2. This agreement also indicates that our calorimeter calibration is reliable. Reference data were, therefore, used for the heat contents of the remaining REE_2O_3 samples in further calculations.

Calorimetry of REE_2O_3 using $3Na_2O{\cdot}4MoO_3$ solvent at 975 K

The sluggish dissolution of REE_2O_3 and REE-bearing compounds in lead borate solvent led to the investigation of $3Na_2O{\cdot}4MoO_3$ as an alternative solvent. A previous study of Y–Zr oxynitrides concluded that there were no dissolution difficulties for Y_2O_3 in sodium molybdate [38].

Table 1 Transposed temperature drop calorimetric experiments, $H_T–H_{298}$ kJ mol^{-1}, for lanthanide sesquioxides. Errors are reported as two standard deviations of the mean. Number of experiments are reported in parentheses. Reference data are reported for comparison (Robie *et al.*, 1979) [37]

Material	$H_T–H_{298}$ (measured)		$H_T–H_{298}$ (literature)	
	T=976 K	T=1078 K	T=976 K	T=1078 K
$LaO_{1.5}$	41.57±0.51(4)	–	42.1	48.9
$NdO_{1.5}$	43.95±0.54(4)	49.06±0.71(4)	44.3	51.7
$SmO_{1.5}$	45.76±0.55(4)	53.67±0.50(4)	45.8	53.3
$EuO_{1.5}$	49.16±1.33(4)	55.23±1.21(5)	47.6	55.3
$GdO_{1.5}$	41.57±0.58(6)	46.68±1.21(4)	41.7	48.3
$HoO_{1.5}$	41.31±0.39(10)	–	42.1	48.8

Enthalpies of drop solution, ΔH_{ds}, for fifteen REE oxides were determined (Table 2) [39]. Experiments were conducted by dropping ≈5 mg pellets into the solvent at calorimeter temperature. Because some of the REE_2O_3 samples are hygroscopic (La_2O_3, Ho_2O_3, Tb_2O_3 and Er_2O_3), these materials were handled in an argon filled glove box to prevent their contamination by water and carbon dioxide. Oxygen was bubbled through the solvent to aid in dissolution by providing constant agitation and to ensure a high oxygen fugacity in the melt in order to maintain a consistent oxidation state of the dissolved REE [40]. Most of REE samples remain trivalent when dissolved. However, Eu^{3+} might conceivably be reduced to Eu^{2+} in the solvent except under oxidizing conditions. The stable cerium oxide under ambient conditions is CeO_2. Previous calorimetric study of Ce_2O_3 indicated that Ce(3+)→Ce(4+) in $2PbO\cdot B_2O_3$ solvent [41]. The current work also confirms that the final state of Ce in $3Na_2O\cdot 4MoO_3$ is tetravalent.

Calorimetry of REE_2O_3 using $2PbO\cdot B_2O_3$ solvent at 1078 K

Enthalpies of drop solution, ΔH_{ds}, in $2PbO\cdot B_2O_3$ at 1078 K were measured for six REE_2O_3 (Table 3). Experiments were conducted in the manner described in the previous section. Furnace tests using $2PbO\cdot B_2O_3$ at 1078 K indicated that dissolution was apparently complete and rapid with a typical reaction time of less than 60 min.

Comparison of solution enthalpy trends

The calculated heat contents were subtracted from the measured ΔH_{ds} values to derive enthalpies of solution, ΔH_s (Table 4). ΔH_s varies linearly with the ionic potential, Z(ionic charge)/r(ionic radius) (Fig. 5). ΔH_s values using $2PbO\cdot B_2O_3$ solvent at 976 K [35] and water at 298.15 K are also shown [42]. All three data sets define sub-parallel

Table 2 Enthalpies of drop solution, ΔH_{ds} kJ mol^{-1}, for lanthanide oxides. Data were collected using $3Na_2O{\cdot}4MoO_3$ solvent at 976 K. Errors are reported as two standard deviations of the mean (Ushakov *et al*., 2001) [39]

$LaO_{1.5}$		CeO_2		$PrO_{1.83}$		$NdO_{1.5}$	
mass/mg	ΔH_{ds}	mass/mg	ΔH_{ds}	mass/mg	ΔH_{ds}	mass/mg	ΔH_{ds}
4.95	–92.91	6.03	70.94	5.08	–40.85	5.25	–85.62
4.88	–94.52	6.17	77.08	5.31	–44.57	4.46	–82.65
4.68	–92.93	5.03	72.98	5.41	–39.81	5.78	–83.08
5.03	–96.47	5.13	73.52	5.54	–42.70	5.03	–78.27
5.34	–97.50	5.55	70.44	4.89	–39.91	4.80	–82.52
5.02	–96.91	5.01	69.26	4.81	–41.42	4.75	–80.69
4.96	–95.68	5.38	76.67	5.54	–40.45	5.39	–82.03
5.21	–95.88	5.57	73.70	5.09	–43.28	6.03	–78.62
–	–	5.71	75.49	4.93	–42.96		
–	–	6.01	73.85	5.29	–40.37		
Average	–95.35		73.39		–41.63		–81.68
Error	1.23		1.65		1.04		1.72
Error/%	1.29		2.24		2.49		2.10

$SmO_{1.5}$		$EuO_{1.5}$		$GdO_{1.5}$		$TbO_{1.5}$	
mass/mg	ΔH_{ds}	mass/mg	ΔH_{ds}	mass/mg	ΔH_{ds}	mass/mg	ΔH_{ds}
5.27	–80.20	5.33	–65.33	4.49	–74.76	5.78	–62.13
5.41	–77.77	4.95	–64.77	5.33	–74.94	5.69	–60.94
5.34	–77.60	5.20	–63.45	4.79	–75.35	5.47	–63.10
5.29	–74.86	5.30	–66.88	5.16	–72.80	5.29	–66.99
5.63	–78.04	4.85	–63.16	5.22	–73.65	5.51	–63.63
4.84	–74.03	4.69	–66.56	5.40	–73.74	5.01	–59.66
4.85	–75.26	5.20	–66.15	4.66	–73.78	5.06	–61.41
4.96	–76.72	5.15	–64.90	4.94	–74.26	5.25	–61.86
5.19	–76.61	5.67	–63.82	4.98	–76.46	4.83	–64.31
4.68	–74.33			4.60	–72.44	5.00	–62.30
						4.69	–64.35
Average	–76.54		–65.00		–74.22		–62.79
Error	1.23		0.90		0.76		1.20
Error/%	1.61		1.39		1.03		1.92

Table 2 Continued

$DyO_{1..5}$		$HoO_{1.5}$		$ErO_{1.5}$		$TmO_{1.5}$	
mass/mg	ΔH_{ds}	mass/mg	ΔH_{ds}	mass/mg	ΔH_{ds}	mass/mg	ΔH_{ds}
5.28	–58.79	6.05	–56.46	5.81	–54.04	5.15	–48.98
5.18	–58.31	5.69	–57.50	5.78	–53.52	5.23	–49.26
5.10	–59.59	5.69	–56.58	6.00	–48.49	5.19	–45.60
5.35	–57.05	5.32	–57.54	4.09	–52.14	5.27	–48.08
5.04	–54.78	5.85	–58.19	6.60	–51.96	6.08	–50.42
5.13	–57.81	6.02	–49.99	3.91	–54.19	5.08	–50.64
4.31	–55.08	6.07	–54.80	5.31	–50.26	5.04	–46.84
5.21	–56.84	6.84	–55.81	5.05	–53.80	5.24	–50.42
5.26	–58.71			4.96	–54.66	5.36	–45.87
				5.06	–53.26	5.07	–49.51
Average	–57.44		–55.86		–52.63		–48.56
Error	1.11		1.84		1.24		1.19
Error/%	1.93		3.29		2.35		2.46

$YbO_{1.5}$		$LuO_{1.5}$		$YO_{1.5}$[1]	
mass/mg	ΔH_{ds}	mass/mg	ΔH_{ds}	mass/mg	ΔH_{ds}
5.24	–53.15	4.72	–46.84	4.22	–62.65
4.45	–52.84	5.20	–48.85	5.69	–65.34
5.04	–49.67	4.77	–48.02	4.68	–59.25
5.32	–49.14	5.56	–48.43	4.68	–61.68
4.94	–51.11	4.72	–47.79	4.32	–59.74
4.91	–51.73	4.58	–50.69	5.02	–60.45
5.06	–47.87	5.85	–47.03		
5.11	–48.67	5.00	–49.96		
4.89	–47.68				
4.74	–46.94				
5.28	–43.28				
4.94	–48.67				
Average	–49.23		–48.45		–61.5
Error	1.59		0.95		1.80
Error/%	3.24		1.96		2.93

[1] Molodetsky, 1999 [33]

Table 3 Enthalpies of drop solution, ΔH_{ds}, for six REE_2O_3 using $2PbO \cdot B_2O_3$ at 1078 K (Risbud *et al.*, 2001 [43]; Zhang, unpublished data). Errors are calculated as two standard deviations of the mean. The number of experiments is in parentheses. Calculated heat contents are reported and are used to calculate the enthalpies of solution, ΔH_s. Reference data are shown for comparison

Material	ΔH_{ds}/kJ mol^{-1} [a]	H_{1078}–H_{298} [b]	ΔH_s/kJ mol^{-1} [c]	ΔH_s/kJ mol^{-1} [d] reference
$LaO_{1.5}$	–13.88±0.09(3)	48.9	–62.8±0.09	–63.0±2.2
$NdO_{1.5}$	–0.05±0.20(2)	51.7	–51.7±0.20	–44.6±2.8
$SmO_{1.5}$	10.90±1.26(8)	53.3	–42.4±1.26	–39.7±2.1
$EuO_{1.5}$	19.78±0.33(3)	55.3	–35.5±0.33	–34.2±0.7
$GdO_{1.5}$	9.75±0.92(4)	48.3	–38.6±0.92	–36.3±1.7
$YO_{1.5}$	18.27±0.75(6)	47.3	–29.0±0.75	–30.9±0.6

[a] Measured; [b] From literature tabulations [41]; [c] Calculated as ΔH_{ds}–(H_{1078}–H_{298}); [d] Measured by solution calorimetry at 976 K [35]

Table 4 Solution enthalpies, ΔH_s, for $REEO_{1.5}$ calculated from enthalpies of drop solution, ΔH_{ds}, and heat content, $\int_{298}^{976} C_p \mathrm{d}T$, calculated using reference C_p data (solvent: $3Na_2O \cdot 4MoO_3$ at 976 K). Reference data for ΔH_s $REEO_{1.5}$ using $2PbO \cdot B_2O_3$ at 976 K are reported for comparison (Takayama–Muramachi and Navrotsky, 1993) [35]. Letters designate the $REEO_{1.5}$ structure type where *A*=hexagonal (*P*3m1), *B*=monoclinic (*C*2/m), *C*=cubic (*I*a3), *F*= cubic (*F*m3m). Numbers of experiments are reported. All values are reported in kJ mol^{-1}

Phase	Structure type	ΔH_{ds} ($3Na_2O \cdot 4MoO_3$)	$\int_{298}^{976} C_p \mathrm{d}T$	ΔH_s ($3Na_2O \cdot 4MoO_3$)	ΔH_s ($2PbO \cdot B_2O_3$)
$YO_{1.5}$	C	–60.37±0.47(9)	40.7	–101.1±0.5	–30.9±0.6
$LaO_{1.5}$	A	–95.35±1.23(8)	42.1	–137.5±1.3	–63.0±2.2
$NdO_{1.5}$	A	–81.68±1.72(8)	44.3	–126.0±1.7	–44.6±2.8
$SmO_{1.5}$	B	–76.81±1.43(8)	45.8	–122.6±1.4	–39.7±2.1
$EuO_{1.5}$	C	–64.62±1.06(8)	47.6	–112.2±1.1	–34.2±0.7
$GdO_{1.5}$	C	–74.27±0.80(10)	41.7	–116.0±0.8	–36.3±1.7
$TbO_{1.5}$	C	–62.79±1.20(11)	44.5	–107.3±1.2	–
$DyO_{1.5}$	C	–57.44±1.11(9)	43.5	–100.9±1.1	–25.5±0.6
$HoO_{1.5}$	C	–55.86±1.84(8)	42.1	–98.0±1.8	–25.1±2.8
$ErO_{1.5}$	C	–52.63±1.24(10)	38.3	–90.9±1.2	–23.8±0.9
$TmO_{1.5}$	C	–48.56±1.19(10)	31.3	–79.9±1.2	–23.6±1.4
$YbO_{1.5}$	C	–49.23±1.59(12)	43.4	–92.6±1.6	–19.8±1.0
$LuO_{1.5}$	C	–48.45±0.95(8)	40.3	–88.8±1.0	–17.2±0.6

trends that describe more than 95% of the variation in the data. ΔH_s for $LaO_{1.5}$ is the most exothermic and ΔH_s for $LuO_{1.5}$ the most endothermic within each trend. All heats of solution are strongly exothermic.

There is excellent agreement between the ΔH_s values measured using $2PbO{\cdot}B_2O_3$ at 976 K and the ΔH_s values calculated from ΔH_{ds} from $2PbO{\cdot}B_2O_3$ at 1078 K and heat contents (Fig. 5, filled circles). The only discrepancy is for $NdO_{1.5}$. The ΔH_s value for $NdO_{1.5}$ calculated using our ΔH_{ds} data and the calculated heat content was 4.3 kJ mol^{-1} more exothermic than the data of Takayama–Muramachi and Navrotsky [35]. The drop solution experiments for $NdO_{1.5}$ yielded very small heat effects (–0.5 kJ mol^{-1}) and were consequently considered less reliable. The 'airgun' solution calorimetry technique was used to check whether the previously reported value for ΔH_s of $NdO_{1.5}$ (–44.6 kJ mol^{-1}) [35] was reproducible. Our measured ΔH_s value of –43.7±3.2 kJ mol^{-1} is equal, within error, to this (Table 3). These results suggest that the ΔH_s for REE_2O_3 remains constant between 976 and 1078 K and that calculating a value for ΔH_{ds} using the ΔH_s and $\int_{298}^{1078} C_p \mathrm{d}T$ is valid and may be used in a thermodynamic cycle using other ΔH_{ds} data.

Thermodynamic cycles and cross-checks: previous studies of REE-materials

Typically two types of thermodynamic cross-checks are employed to ensure the accuracy of calorimetric data [27, 29, 34]. The first compares enthalpies of formation, ΔH_f, calculated using measured data to reference values; thus, providing direct evidence of data accuracy by independent means. This type of cross-check is only as

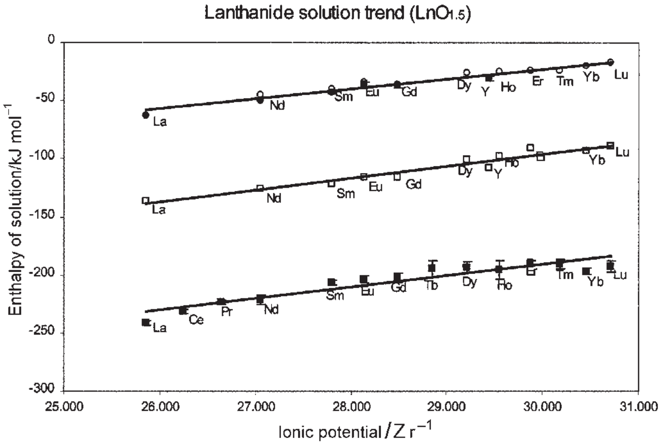

Fig. 5 Solution enthalpies for $REEO_{1.5}$ in three solvents: $3Na_2O{\cdot}4MoO_3$ at 975 K (open squares), $2PbO{\cdot}B_2O_3$ at 975 (open circles) and 1078 K (filled circles) and water at 298.15 K (filled squares)

good as the reference data it relies on. Comparisons must always be made carefully and sources of reference data must be checked for accuracy [39]. Our experience is that tabulated data are not always as reliable as one might, at first glance, assume. The second technique used to cross-check calorimetric data relies on the different chemical/structural properties of the two oxide solvents. Parallel studies are conducted using borate and molybdate solvents. If there is consistency of calculated ΔH_f values using two independent thermodynamic cycles, this is taken as evidence that the final states of the materials studied within each solvent are reproducible and their use in thermodynamic cycles is valid.

Several recent studies examined the energetics of REE-bearing compounds and provided thermodynamic cross-checks that validate our calorimetric techniques for REE_2O_3 [38–41, 43]. We discuss here calorimetric studies of two classes of materials, REE orthophosphates, and REE silicate-oxyapatites.

Rare earth orthophosphates

The REE-orthophosphates, $REEPO_4$, are widely used in technical applications as scintillators for gamma-ray detection [44–47], thermophosphors and hosts for microlasers [22–24]. A recent study was conducted to derive enthalpies of formation, ΔH_f^0, for several $REEPO_4$, where *REE*= Sc, Y, La–Nd, Sm–Lu. Enthalpies of drop solution, ΔH_{ds}, using $3Na_2O{\cdot}4MoO_3$ at 975 K were measured and used with the data in Table 1 in thermodynamic cycles to calculate enthalpies of formation from the oxides, ΔH_{f-ox}^0, and from the elements, (Table 5) [39]. One representative thermodynamic cycle is shown to illustrate the process (Table 6). A plot of the ΔH_{ds} for the $REEPO_4$ samples as a function of ionic potential (*Z*/*r*) reveals that $CePO_4$ falls off the trend in an exothermic direction (Fig. 6). This is consistent with oxidation of Ce(III) to Ce(IV) in $3Na_2O{\cdot}4MoO_3$ solvent because oxidation reactions are strongly exothermic. The enthalpies of formation from the oxides when plotted *vs.* the ionic potential (*Z*/*r*) of the REE cation define a linear trend (Fig. 7). $LaPO_4$ has the most exothermic ΔH_{f-ox}^0 and $LuPO_4$ the least All $REEPO_4$ samples are energetically stable with respect to their oxides.

Two types of thermodynamic cross-checks were used to verify the accuracy of the $REEPO_4$ enthalpy data [39]. The first was a parallel study using $2PbO{\cdot}B_2O_3$ solvent at 976 K. Three orthophosphates, $LuPO_4$, YPO_4 and $LaPO_4$, were used in the lead borate study and their enthalpies of formation from the oxides, ΔH_{f-ox}^0, were calculated and compared to the data derived using $3Na_2O{\cdot}4MoO_3$ (Table 7). There was excellent agreement among the data. The second type of thermodynamic cross-check involved a comparison of the Ushakov *et al.* data [39], derived from high temperature oxide melt calorimetry, to previously reported values.These values for standard enthalpies of formation, ΔH_f^0, for $REEPO_4$ were calculated from their solubilities in aqueous acid and one value was obtained using acid solution calorimetry. They define a roughly parallel but more endothermic trend compared to the Ushakov *et al.* data (Table 8) [39]. Such an effect may reflect discrepancies in the thermodynamic properties of aqueous species used in the derivation of standard state properties from

Table 5 Enthalpies of drop solution, ΔH_{ds}, in $3Na_2O{\cdot}4MoO_3$ at 976 K and enthalpies of formation from the oxides, ΔH^0_{f-ox}, and from the elements, ΔH^0_f, for REEPO$_4$ (Ushakov *et al.*, 2001) [39]. Number of experiments are reported

Phase	ΔH_{ds}/kJ mol^{-1}	ΔH^0_{f-ox}/kJ mol^{-1}	ΔH^0_f/kJ mol^{-1}
YPO_4	139.97±1.13(7)	–282.6±1.3	–1987.7±1.7
$LaPO_4$	143.73±0.89(11)	–321.4±1.6	–1970.7±1.8
$CePO_4$	112.28±0.84(10)	–317.2±4.8	–1967.8±2.4
$PrPO_4$	137.20±1.13(7)	–312.2±5.0	–1969.5±3.7
$NdPO_4$	147.98±1.33(9)	–312.0±2.2	–1968.4±2.3
$SmPO_4$	142.66±1.54(8)	–301.8±2.1	–1965.7±2.4
$EuPO_4$	139.87±1.43(6)	–286.8±1.8	–1870.6±2.6
$GdPO_4$	139.65±0.92(9)	–296.2±1.3	–1962.2±4.4
$TbPO_4$	140.98±1.39(9)	–286.1±1.9	–1971.1±4.6
$DyPO_4$	144.14±1.23(10)	–283.9±1.7	–1967.9±2.6
$HoPO_4$	140.64±1.43(13)	–278.8±2.4	–1971.6±3.4
$ErPO_4$	140.62±1.35(7)	–275.6±1.9	–1976.9±2.1
$TmPO_4$	137.10±1.59(9)	–268.0±2.0	–1964.7±4.7
$YbPO_4$	138.05±1.69(10)	–269.6±2.4	–1929.4±4.9
$LuPO_4$	133.14±1.55(10)	–263.9±1.9	–1955.4±4.2

Table 6 A representative thermodynamic cycle for calculating for REEPO$_4$ using data derived using $3Na_2O{\cdot}4MoO_3$ solvent at 976 K

Reaction		ΔH/kJ mol^{-1}
(1) ΔH_{ds}	$LaPO_{4\,(s,\,298)} \rightarrow LaO_{1.5\,(sln,\,976)} + 1/2P_2O_{5\,(sln,\,976)}$	143.73±0.89
(2) ΔH_{ds}	$LaO_{1.5\,(s,\,298)} \rightarrow LaO_{1.5\,(sln,\,976)}$	–95.35±1.23
(3) ΔH_{ds}	$P_2O_{5\,(s,\,298)} \rightarrow P_2O_{5\,(sln,\,976)}$	–164.60±0.85
(4) ΔH^0_{f-ox}	$LaO_{1.5\,(s,\,298)} + 1/2\ P_2O_{5\,(s,\,298)} \rightarrow LaPO_{4\,(s,\,298)}$	–321.4±1.6
$\Delta H(4) = -\Delta H(1)+\Delta H(2)+1/2\Delta H(3)$		

Table 7 Thermodynamic cross check of the enthalpies of formation from the oxides, ΔH^0_{f-ox}, for three REE-orthophosphates. Data were derived using two solvents, $3Na_2O{\cdot}4MoO_3$ and $2PbO{\cdot}B_2O_3$ at 976 K (Ushakov *et al.*, 2001) [39]

Phase	ΔH^0_{f-ox}/kJ mol^{-1} $3Na_2O{\cdot}4MoO_3$	ΔH^0_{f-ox}/kJ mol^{-1} $2PbO{\cdot}B_2O_3$
$LaPO_4$	–321.4±1.6	–325.9±2.6
YPO_4	–282.6±1.3	–280.4±1.5
$LuPO_4$	–263.9±1.9	–262.7±1.6

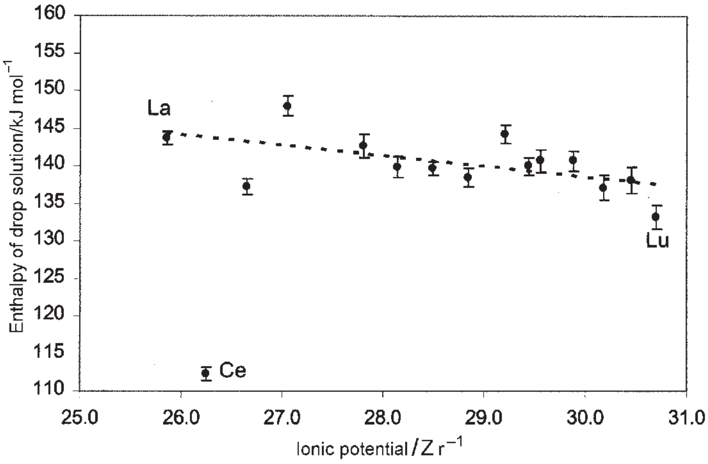

Fig. 6 Enthalpies of drop solution, ΔH_{ds}, in $3Na_2O{\cdot}4MoO_3$ at 975 K *vs.* ionic potential (*Z*/*r*) for $REEPO_4$. The trend is approximately linear with $CePO_4$ falling off the trend in an exothermic direction. This is consistent with oxidation of Ce(III) to Ce(IV) in $3Na_2O{\cdot}4MoO_3$

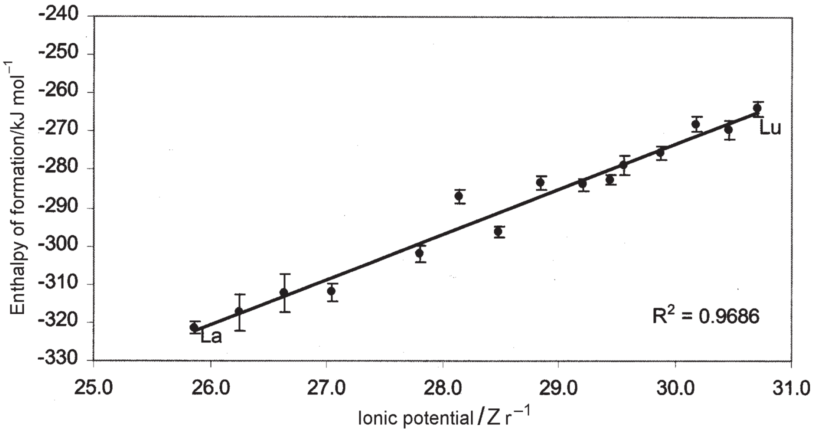

Fig. 7 Enthalpies of formation from the oxides, ΔH^{0}_{f-ox}, *vs.* ionic potential (*Z*/*r*) for $REEPO_4$. Data derived using $3Na_2O{\cdot}4MoO_3$ solvent at 975 K. The linear trend accounts for nearly 97% of the variation in the data

aqueous data. The Ushakov *et al.* values for of La-, Ce- and $PrPO_4$ are, within error, equal to those derived using acid solubility data [48–51]. Vaporization studies of $REEPO_4$ using mass spectrometry combined with Knudsen effusion were also reported [52, 53]. The only data point from the Ushakov *et al.* study that is consistent with the vaporization data is of $LuPO_4$. In order for the vaporization studies to yield accurate results, complete sample decomposition must be achieved according to the reaction: $2REEPO_4 \rightarrow REE_2O_3+2PO_2+1/2O_2$. However, the formation of oxyphosphates upon P_2O_5 vaporization at high temperatures can not be ruled out [54, 55]. The error introduced by not achieving a reproducible final state is expected to be more significant for the light $REEPO_4$ because they are more refractory [56, 57]. For this reason the discrepancies between the Ushakov *et al.* data and the vaporization studies is not surprising [39].

Table 8 The standard enthalpies of formation, ΔH_f^0, for three orthophosphates. All values are reported in kJ mol^{-1} (Ushakov *et al.*, 2001) [39]

Phase	ΔH_f^0/kJ mol^{-1}	Reference, method of determination
$LaPO_4$	–1913±10	mass spectrometric plus Knudsen effusion[1]
	–1949±4	$LaCl_3+H_3PO_4$ reaction calorimetry[2]
	–1962±8	calculated from solubility in HCl[2,3]
	–1970.7±1.8	high temperature oxide melt calorimetry[4]
$CePO_4$	–1897±31	mass spectrometric plus Knudsen effusion[5]
	–1955	calculated from solubility in HCl[3]
	–1963	calculated using solubility data[6,7]
	–1967.8±2.4	high temperature oxide melt calorimetry[4]
YPO_4	–1953±8	calculated from solubility in HCl[2]
	–1966±8	$YCl_3+H_3PO_4$ reaction calorimetry[2]
	–1987.7±1.7	high temperature oxide melt calorimetry[4]

[1]Rat'kovskii *et al.*, 1973 [52]; [2]Marinova *et al.*, 1973 [48]; [3]Marinova *et al.*, 1976 [49]; [4]Ushakov *et al.*, 2001 [39]; [5]Balducci *et al.*, 1978 [53]; [6]Almendra and Ogasawara, 1996 [50]; [7]Firsching and Brune, 1991 [51]

This study of rare earth orthophosphates is a good example of how to apply multiple thermodynamic cross-checks to calorimetric data in order to verify their accuracy. This study also illustrates the need to critically assess reference values to ensure that a fair comparison is made. We conclude that the directly measured heats of formation are more reliable than the earlier less direct estimates.

Rare earth oxyapatites

Rare earth oxyapatites, $REE_{9.33}\square_{0.67}(SiO_4)_6O_2$, where *REE*=La, Sm, Nd, Gd, $\square$ = vacancy, have many interesting technical applications. Rare earth oxides are used as sintering aids during the processing of silicon nitride ceramics resulting in REE-oxyapatite formation at grain triple junctions [25]. There is also interest in Gd-bearing compounds because of their high luminescence efficiency when doped with other rare earth ions [58–60]. Many of these properties can be attributed to the oxyapatite structure that contains oxygen atoms isolated from the Si-tetrahedra. These oxygen atoms occupy channels in the structure parallel to the *c*-axis and are loosely bonded to REE cations in the framework [61]. Thermodynamic measurements are necessary for assessing the phase stability of the REE-oxyapatites in these applications [43].

Enthalpies of drop solution, ΔH_{ds}, for four REE-oxyapatites were collected using $2PbO\cdot B_2O_3$ solvent at 1078 K (Table 9) [43]. These data along with data from Table 3 and the ΔH_{ds} value for SiO_2, quartz, 49.8±1.0 kJ mol^{-1}, were used in thermodynamic cycles (Table 10) to calculate the enthalpies of formation from the oxides, ΔH^0_{f-ox}, and the standard enthalpy of formation, (Table 11). The absolute errors reported for the ΔH_{ds} values for the

Table 9 Enthalpies of drop solution, ΔH_{ds}, for $REE_{9.33}\square_{0.67}(SiO_4)_6O_2$ in $2PbO\cdot B_2O_3$ at 1078 K. Values are reported in kJ mol^{-1} and errors are calculated as two standard deviations of the mean. Number of experiments are reported in (Risbud *et al.*, 2001) [43]

Phase	ΔH_{ds}/kJ mol^{-1}	Relative error/%
$Gd_{9.33}\square_{0.67}(SiO_4)_6O_2$	837.2±21.4(10)	2.6%
$Sm_{9.33}\square_{0.67}(SiO_4)_6O_2$	989.9±17.1(7)	1.7%
$Nd_{9.33}\square_{0.67}(SiO_4)_6O_2$	1056.5±31.8(5)	3.0%
$La_{9.33}\square_{0.67}(SiO_4)_6O_2$	933.2±23.3(4)	2.5%

Table 10 The thermodynamic cycle used for the calculation of the enthalpies of formation from the oxides for REE-oxyapatite (*REE*=Gd, Sm,Nd, La) (Risbud *et al.*, 2001) [43]

(1) ΔH_{ds} $REE_2O_{3\ (crystal,\ 298\ K)} \rightarrow REE_2O_{3\ (sol,\ 1078\ K)}$

(2) ΔH_{ds} $SiO_{2\ (crystal,\ 298\ K)} \rightarrow SiO_{2\ (sol,\ 1078\ K)}$

(3) ΔH_{ds} $REE_{9.33}\square_{0.67}(SiO_4)_6O_{2\ (crystal,\ 298\ K)} \rightarrow 14/3REE_2O_{3(sol,\ 1078\ K)} + 6SiO_{2(sol,\ 1078\ K)}$

(4) $\Delta H^0_{f-ox} = 14/3\Delta H(1) + 6\Delta H(2) - \Delta H(3)$

Table 11 The and the standard enthalpy of formation, ΔH^0_f, for REE-oxyapatite phases kJ mol^{-1}. Errors are propagated assuming linear combinations of independent variables (Risbud *et al.*, 2001) [43]

Phase	ΔH^0_{f-ox}/kJ mol^{-1}	ΔH^0_f/kJ mol^{-1}
$Gd_{9.33}\square_{0.67}(SiO_4)_6O_2$	–446.9±21.9	–14402.7±28.2
$Sm_{9.33}\square_{0.67}(SiO_4)_6O_2$	–589.4±23.2	–14561.7±20.8
$Nd_{9.33}\square_{0.67}(SiO_4)_6O_2$	–715.7±32.4	–14616.8±32.2
$La_{9.33}\square_{0.67}(SiO_4)_6O_2$	–764.1±23.4	–14599.6±26.1

$REE_{9.33}\square_{0.67}(SiO_4)_6O_2$ samples were large, ranging from 17 to 31 kJ mol^{-1}. The increased error is attributed mainly to the very large molecular mass of this compound whose formula contains 26 oxygen atoms. Sample heterogeneity may also increase the scatter. Because the ΔH_{ds} values for the $REE_{9.33}\square_{0.67}(SiO_4)_6O_2$ samples are also very large (>800 kJ mol^{-1}) the relative errors are acceptable and typical of slightly heterogeneous samples ranging (1.7 to 3.0%). When was plotted *vs*. the ionic potential (*Z*/*r*) of the REE-ion a notably non-linear trend was observed (Fig. 8).

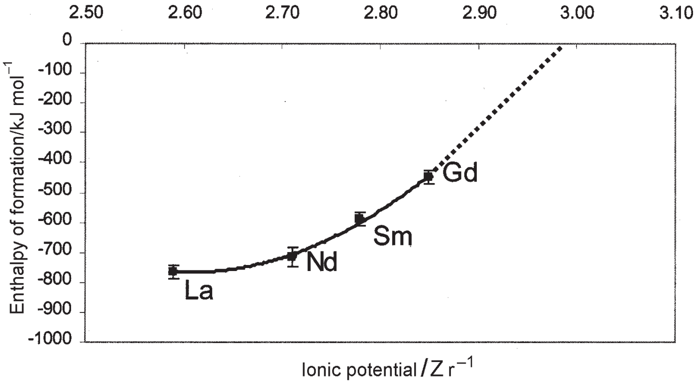

Fig. 8 The enthalpies of formation from the oxides, $\Delta H^0_{\mathrm{f-ox}}$, for REE-oxyapatites plotted *vs*. the ionic potential (*Z*/*r*) of the REE-ion. The dotted line represents an extrapolation of the fitted data (Risbud *et al.*, 2001) [43]

Three conclusions were drawn. First, all of the REE-oxyapatites studied are stable with respect to their binary oxides. Second, the enthalpy trend as a function of ionic potential (*Z*/*r*) indicated that the REE-oxyapatites become more energetically stable as the ionic potential decreases, i.e. as the ionic radius of the REE-ion becomes larger (Fig. 8). Conversely, decreasing the ionic-radii beyond Gd destabilizes the oxyapatite phase allowing for the possible formation of competing REE-silicate structures [43]. Third, the stabilization effect of increasing ionic radii of the REE ion is not a linear function of radius. Relatively little additional stabilization of the oxyapatite structure is gained by increasing the ionic radii of the REE-ion beyond Nd as shown by a flattening of the enthalpy curve (Fig. 8). For the REE-oxyapatites, substituting Sm for Gd stabilizes the structure by, presumably, better satisfying the bonding requirements of the REE-site in this complex silicate. This stabilization effect may continue until the REE-site ion becomes too large and begins to destabilize the structure. The eventual destabilization of the structure is not seen experimentally, as there is no trivalent ion with ionic radius greater than lanthanum [43]. The importance of this observation is that it reveals a potential pitfall with predictions of thermodynamic properties by extrapolating linearly beyond experimental data [62].

Recommended techniques for high temperature oxide melt solution calorimetric investigations of REE-materials

Our experience with REE_2O_3 and REE ternary compounds suggest the following:
(1) $3Na_2O{\cdot}4MoO_3$ solvent at 976 K is excellent for both solution and drop solution

experiments for binary REE_2O_3 and for multicomponent compounds containing other highly charged cations (Ti, Zr, P), but it does not readily dissolve Al_2O_3 and SiO_2. (2) $2PbO{\cdot}B_2O_3$ near 1078 K works well in both solution and drop solution mode for both binary and multicomponent REE_2O_3 – containing compounds. (3) Dissolution difficulties make lead borate somewhat problematic for REE_2O_3 near 976 K, though less refractory multicomponent oxides dissolve better. (4) When ΔH_{ds} is too small to be measured accurately (because of compensation of endothermic heat content and exothermic heat of solution), then solution calorimetric methods are appropriate. The effect of stirring must be subtracted from the measured enthalpy as a correction. This correction is about 0.6 to 0.8 J per experiment, so if the sample does not contribute 8–10 J, the stirring correction may contribute too much uncertainty. A recent advance in the design of the solution sample holder, the so-called ‘airgun’ sample holder has a much faster equilibration time (≈1.5 h) and allows for the collection of four to six data points per day. There is also no need to apply a stirring correction. The disadvantage is that the sample must be pelletized. (5) The mixing of sample with a diluent to aid its dissolution is to be avoided. A better way to deal with sluggish dissolution of some samples in $2PbO{\cdot}B_2O_3$ at 976 K is to perform experiments near 1078 K, or to use $3Na_2O{\cdot}4MoO_3$ at 976 K instead. (Note that the sodium molybdate solvent is not recommended for use at 1078 K because of the high vapor pressure of MoO_3.)

Conclusions

Whether using $3Na_2O{\cdot}4MoO_3$ or $2PbO{\cdot}B_2O_3$ solvent, each experimentalist must investigate the efficacy of the approaches recommended here as they pertain to specific materials. Furnace tests and where possible, EMPA of quenched solvents, should be conducted. Furnace tests give an indication of the dissolution characteristics of the material in a given solvent at a given temperature. These tests must be conducted for both binary and ternary compounds. The absence of undissolved particles or reaction products in quenched $2PbO{\cdot}B_2O_3$ solvent as detected by EMPA is excellent evidence that dissolution is achieved. These recommendations should be taken as guidelines, and not as a prescription, for calorimetry of REE-materials. Each new system requires careful attention to technique.

* * *

This work supported by the US Department of Energy Basic Energy Sciences (DEFG02-97ER45656) and Environmental Management Science Program (DEFG07-97ER45673).

References

1 P. Moller, Lanthanoids as a geochemical probe and problems in lanthanoid, geochemistry. Distribution and behavior of lanthanoids in non-magmatic phases, in Systematics and the Properties of the Lanthanides (Ed. S. P. Sinha), Reidel Publishing Co., NATO ASI Series, 1983, p. 561.
2 P. Henderson, Rare Earth Element Geochemistry, Elsevier, 1984, p. 510.

3 B. R. Lipin and G. A. McCay (Eds), Reviews in Mineralogy, 21, Mineralogical Society of America, 1989, p. 348.

4 J. C. G. Bunzli and G. R. Choppin (Eds), Lanthanide Probes in Life, Chemical and Earth Sciences. Theory and Practice, Elsevier, 1989, p. 432.

5 A. P. Jones, F. Wall and C. T. Williams (Eds), Rare Earth Minerals. Chemistry, Origin and Ore Deposits: The Mineralogical Society Series, 7, Chapman and Hall, 1996, p. 372.

6 GEOREF, www.csa.com: internet database service, geology and geophysics from 1785 to present.

7 A. F. Wells, Structural Inorganic Chemistry, Clarendon Press, New York, Oxford University Press 1984, p. 1382.

8 G. A. McCay, Geochemistry and Mineralogy of Rare Earth Elements: Reviews in Mineralogy, 21, Mineralogical Society of America, 1989, p. 45.

9 D. G. Brookins, Geochemistry and Mineralogy of Rare Earth Elements: Reviews in Mineralogy, 21, Mineralogical Society of America, 1989, p. 201.

10 S. M. McLennan, Geochemistry and Mineralogy of Rare Earth Elements: Reviews in Mineralogy, 21, Mineralogical Society of America, 1989, p. 169.

11 W. V. Boynton, Geochemistry and Mineralogy of Rare Earth Elements: Reviews in Mineralogy, 21, Mineralogical Society of America, 1989, p. 1.

12 N. M. Evensen, P. J. Hamilton and R. K. O'Nions, Geochim. Cosmochim. Acta, 42 (1978) 1199.

13 E. Anders and M. Ebihara, Geochim. Cosmochim. Acta, 46 (1982) 2363.

14 S. R. Taylor and S. M. McLennon, The Continental Crust: Its Composition and Evolution, Blackwell 1985, p. 312.

15 H. A. Liebhafsky and E. J. Cairns, Fuel Cells and Fuel Batteries, Wiley and Sons, New York 1968, p. 435.

16 S. Kartha and P. Grimes, Physics Today, 11 (1994) 54.

17 F. T. Ciacchi, K. M. Crane and S. P. S. Badwal, Solid State Ionics, 73 (1994) 49.

18 N. J. Kleykamp, J. Nucl. Mater., 275 (1999) 1.

19 Hj. Matzke, V. V. Rondinella and T. Wiss, J. Nucl. Mater., 274 (1999) 47.

20 K. Bakker, H. Hein, R. J. M. Konings, R. R. Van der Laan, Hj. Matzke and P. J. Van Vlaanderen, J. Nucl. Mater., 252 (1998) 228.

21 N. P. Raju, M. Dion, M. J. P. Gingras, T. E. Mason and J. E. Greedan, Physical Review B, 59 (1999) 14489.

22 S. W. Allison, L. A. Boatner and G. T. Gillies, Appl. Opt., 25 (1995) 5624.

23 A. Rapaport, V. Davis, M. Bass, C. Deka and L. A. Boatner, J. Lumin., 85 (1999) 155.

24 A. Rapaport, O. Moteau, M. Bass, L. A. Boatner and C. Deka, J. Opt. Soc. Amer. B, 16 (1999) 911.

25 K. P. Plucknett and D. S. Wilkinson, J. Mater. Res., 10 (1995) 1387.

26 F. W. Walker, J. R. Parrington and F. Feiner, Nuclides and Isotopes, 14th ed. General Electric Nuclear Energy, 1989, p. 57.

27 A. Navrotsky, Phys. Chem. Min., 2 (1977) 89.

28 A. Navrotsky, Phys. Chem. Min., 24 (1997) 222.

29 A. Navrotsky, R. P. Rapp, E. Smelik, P. Burnley, S. Circone, L. Chai, K. Bose and H. R. Westrich, Amer. Mineral., 79 (1994) 1099.

30 J. M. McHale, G. R. Kowach, A. Navrotsky and F. J. DiSalvo, Chem. Eur. J., 2 (1996) 1514.

31 I. Molodetsky, A. Navrotsky, M. Lajavardi and A. Brune, Z. Physical Chem., 207 (1998) 59.

32 J. Liang, A. Navrotsky, T. Ludwig, H. J. Seifert and F. Aldinger, J. Mater. Res., 14 (1999) 1.

33 I. Molodetsky, Ph.D. Dissertation, Princeton University, 1999, p. 233.
34 S. V. Ushakov and K. Grevel, personal communication, 2001.
35 E. Takayama-Muramachi and A. Navrotsky, J. Solid State Chem., 106 (1993) 349.
36 J. Bularzik, A. Navrotsky, J. Bringley, B. Scott and S. Trail, J. Solid State Chem., 93 (1991) 418.
37 R. A. Robie, B. S. Hemingway and J. R. Fisher, U.S. Geol. Surv. Bull. 1452, Washington, D.C., 1979.
38 I. Molodetsky, A. Navrotsky, F. DiSalvo and M. Lerch, J. Mater. Res., 15 (2000) 2558.
39 S. V. Ushakov, K. B. Helean, A. Navrotsky and L. A. Boatner, J. Mater. Res., 16 (2001) 2623.
40 A. Navrotsky, J. Therm. Anal. Cal., 57 (1999) 653.
41 R. L. Putnam, A. Navrotsky, E. H. P. Cordfunke and M. E. Huntelaar, J. Chem. Therm., 32 (2000) 911.
42 L. R. Morss, J. Less-Common Metals, 93 (1983) 301.
43 A. S. Risbud, K. B. Helean, M. C. Wilding, P. Lu and A. Navrotsky, J. Mater. Res., 16 (2000) in press.
44 W. W. Moses, M. J. Weber, S. E. Derezno, D. Perry, P. Berdahl and L. A. Boatner, IEEE Trans. Nucl. Sci., 45 (1998) 462.
45 A. J. Wojtowicz, D. Wisniewski, A. Lempicki and L. A. Boatner, Radiation Effects and Defects in Solids, 135 (1995) 305.
46 A. J. Wojtowicz, D. Wisniewski, A. Lempicki and L. A. Boatner, Mater. Res. Soc. Symp. Proc., 348 (1994) 305.
47 A. Lempicki, E. Berman, A. J. Wojtowicz, M. Balcerzyk and L. A. Boatner, IEEE Trans. Nucl. Sci., 40 (1993) 384.
48 L. A. Marinova, V. P. Glibin and A. I. Volkov, Rassh. Tezisi Dokl. Tbilissi, Meznierba, 71 (1973) 203.
49 L. A. Marinova and V. N. Yaglov, Zh. Fiz. Khim., 50 (1976) 802.
50 E. R. Almendra and T. Ogasawara, Congr. Anu.- Assoc. Bras. Metal Mater., 50 (1996) 1.
51 F. H. Firsching and S. N. Brune, J. Chem. Eng. Data, 36 (1991) 93.
52 I. A. Rat'kovskii, B. A. Botylin and G. I. Novikov, Dokl. Akad. Nauk. Beloruss. SSR, 17 (1973) 232.
53 G. Balducci, G. De Maria, G. Gigli and M. Guido, Adv. Mass Spectrom., 7A (1978) 651.
54 J. J. Serra, J. Coutures and A. Rouanet, High Temp.-High Press., 8 (1976) 337.
55 A. Rouanet, J. J. Serra, K. Allaf and V. P. Orlovskii, Izv. Akad. Nauk SSSR, Neorg. Mater., 17 (1981) 104.
56 Y. Hikichi and V. J. Nomura, J. Amer. Ceram. Soc., 70 (1987) C-252.
57 Y. Hikichi, T. Ota, K. Daimon and V. Hattori, J. Amer. Ceram. Soc., 81 (1998) 2216.
58 J. Lin and Q. Su, J. Alloys Cmpds., 210 (1994) 159.
59 J. Lin and Q. Su, Phys. Stat. Sol.(b), 196 (1996) 261.
60 C. R. Ronda, T. Justel and H. Nikol, J. Alloys Cmpds., 255-277 (1998) 669.
61 A. N. Christiansen, R. G. Hazell and A. W. Hewat, Acta. Chem. Scand., 51 (1997) 37.
62 A. Navrotsky, Ceram. Trans., 107 (2000, in press).